

# Internal Electron Transfer in Cytochrome *c* Oxidase: Evidence for a Rapid Equilibrium between Cytochrome *a* and the Bimetallic Site<sup>†</sup>

Mikael Oliveberg and Bo G. Malmström\*

Department of Biochemistry and Biophysics, Chalmers University of Technology and University of Göteborg, S-412 96 Göteborg, Sweden

Received February 6, 1991; Revised Manuscript Received April 24, 1991

**ABSTRACT:** Internal electron-transfer reactions in cytochrome oxidase following flash photolysis of the CO compounds of the enzyme reduced to different degrees (2–4 electron equiv) have been followed at 445, 605, and 830 nm. Apart from CO dissociation and recombination, two kinetic phases are seen both at 445 and at 605 nm with rate constants of  $2 \times 10^5$  and  $1.3 \times 10^4$  s<sup>-1</sup>, respectively; at 605 nm, an additional phase with a rate constant of 400 s<sup>-1</sup> is resolved. At 830 nm, only the second reaction phase (rate constant of  $1.3 \times 10^4$  s<sup>-1</sup>) is observed. The amplitude of the first phase is largest with the two-electron-reduced enzyme, whereas that of the second phase is maximal at the three-electron-reduction level. Neither phase shows any marked pH dependence. The reaction in the first phase has a free energy of activation of 41 kJ mol<sup>-1</sup> and an entropy of activation of  $-14$  J K<sup>-1</sup> mol<sup>-1</sup>. Analysis suggests that the two rapid reaction phases represent internal electron redistributions between the bimetallic site and cytochrome *a*, and between cytochrome *a* and Cu<sub>A</sub>, respectively. The slow phase (400 s<sup>-1</sup>) probably involves a structural rearrangement.

Cytochrome *c* oxidase, the terminal complex of the mitochondrial respiratory chain, is a redox-linked proton pump [see Wikström et al. (1981)]. It contains four redox-active metal centers: two heme groups (cytochromes *a* and *a*<sub>3</sub>), and two copper ions (Cu<sub>A</sub> and Cu<sub>B</sub>). Cytochrome *a*<sub>3</sub> and Cu<sub>B</sub> form a bimetallic unit, which constitutes the dioxygen-reducing site. Electrons from cytochrome *c* initially reduce cytochrome *a* and Cu<sub>A</sub> and are then transferred intramolecularly to the bimetallic site.

Information on the kinetics of the intramolecular electron-transfer reactions involving the four redox sites is of obvious importance to a mechanistic understanding of the electron transfer from cytochrome *c* to dioxygen and the coupling of this reaction to proton translocation. For example, it is still not known whether cytochrome *a* or Cu<sub>A</sub> is the primary electron acceptor [see Malmström (1990)], even if some recent work (Kobayashi et al., 1989; Hill, 1991) favors Cu<sub>A</sub>. In either case, however, both become rapidly reduced if the redox equilibrium between these sites is rapid. Furthermore, it is not established if only one of these sites can transfer electrons to the bimetallic site, or if there are parallel pathways. Finally, the coupling between electron transfer and proton translocation requires a structural modulation of some internal electron-transfer step ("electron gating") (Blair et al., 1986a).

Some information on the kinetics of internal electron transfer has been derived from studies with the two- and three-electron-reduced enzyme. Binding of CO to these enzyme forms stabilizes the reduced bimetallic site with the other two sites either fully oxidized or just partially reduced. Dissociation of the CO from the complexes by a short laser flash induces an electron redistribution between the redox sites (Boelens et al., 1982; Brzezinski & Malmström, 1987; Morgan et al., 1989). In this way, evidence has been provided that there is a facile electron transfer between the bimetallic site and Cu<sub>A</sub> (Boelens et al., 1982; Brzezinski & Malmström, 1987), and also between Cu<sub>A</sub> and cytochrome *a* (Morgan et al., 1989).

In this paper, we describe an extension of the earlier work in which we use a laser system with an improved time resolution and a better detection system in the near-infrared. Our measurements confirm the earlier observations, but we have also found an initial phase which is faster than any seen previously. We argue that this phase represents a redox equilibrium between cytochrome *a* and the bimetallic site. This reaction does not have a pronounced pH dependence, but the temperature dependence is considerable.

## MATERIALS AND METHODS

Cytochrome oxidase was prepared from bovine hearts by the method of Van Buuren (1972). Cytochrome *c* was isolated from horse hearts by the procedure of Brautigan et al. (1978) and then further purified by ion-exchange chromatography. The buffer used in all experiments was 50 mM 4-(2-hydroxyethyl)-1-piperazineethanesulfonic acid (Hepes)<sup>1</sup> containing 0.167 M K<sub>2</sub>SO<sub>4</sub> and 0.5% Tween 80; K<sub>2</sub>SO<sub>4</sub> was included to keep the ionic strength constant in the pH studies.

**Sample Preparation.** The frozen stock enzyme was thawed and immediately transferred to a modified Thunberg cuvette containing the buffer. The cuvette was then evacuated and flushed with CO. At room temperature, the mixed-valence-state cytochrome oxidase was formed within 12 h. To obtain the three-electron-reduced species, the mixed-valence enzyme was titrated with ascorbate, TMPD, and cytochrome *c*. The degree of reduction was determined from the absorption spectrum in the region 550–650 nm.

It was noted that the enzyme incubated under CO sometimes took more than two electrons, particularly at high pH. To avoid this in the mixed-valence-state experiments, some of these were carried out after a few hours incubation, so that a small part of the enzyme population was still fully oxidized.

**Photolysis.** A Nd-YAG laser from Quantel was used for the photolytic dissociation of CO. Its output wavelength was 532 nm, the duration of the pulse 9 ns, and the total energy about 0.3 J. The analysis light used in the visible region of

<sup>†</sup> This work was supported by grants from the Swedish Natural Science Research Council and the Knut and Alice Wallenberg Foundation.

<sup>1</sup> Abbreviations: Hepes, 4-(2-hydroxyethyl)-1-piperazineethanesulfonic acid; TMPD, tetramethyl-*p*-phenylenediamine.

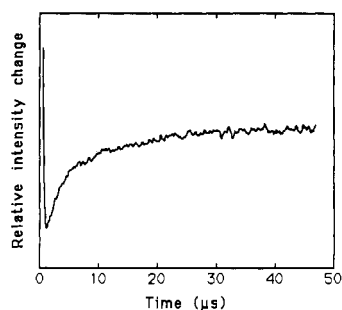


FIGURE 1: Time course of the intensity changes at 445 nm following flash photolysis of mixed-valence carboxycytochrome oxidase ( $5 \mu\text{M}$ ). Since the intensity represents transmission, absorbance increases correspond to downward deflections, and vice versa, in this figure as well as in Figures 2 and 3.

Table I: Absorbance Changes following Flash Photolysis of Carboxycytochrome Oxidase<sup>a</sup>

enzyme form	reaction phase <sup>b</sup>	absorbance change $\times 10^3$ at		
		445 nm	605 nm	830 nm
mixed valence	1st	-34	+4.8	
	2nd	-13	-1.3	-0.2
3-e <sup>-</sup> -reduced	1st	-21	+3.4	
	2nd	-23	-4.8	-0.7

<sup>a</sup>The oxidase concentration was  $5 \mu\text{M}$  except in the 830-nm measurements, where it was  $30 \mu\text{M}$ . <sup>b</sup>The first phase has a rate constant of approximately  $2 \times 10^5 \text{ s}^{-1}$  and the second one  $1.3 \times 10^4 \text{ s}^{-1}$ .

the spectrum came from a 250-W halogen lamp in combination with a heat filter and three monochromators. The light intensity changes were determined by Hamamatsu photomultipliers R 269 and R 712. At 830 nm, a solid-state laser with corresponding photodiode was used to follow the absorbance changes. The experimental traces represent an averaging of about 20 recordings.

The recorded transients were fitted to a sum of first-order exponentials using the Levenberg-Marquardt nonlinear least-squares method.

## RESULTS

At 445 and 605 nm, the mixed-valence and three-electron-reduced enzymes display comparatively large absorbance changes due to the photolysis and recombination of CO. Despite this fact, it is possible to resolve relaxations of the internal electron equilibria during this process.

Figure 1 shows the initial absorbance changes at 445 nm of the mixed-valence enzyme after CO photolysis. The first phase of the absorbance decrease has an apparent rate constant of  $2.7 \times 10^5 \text{ s}^{-1}$ , and it is followed by a further decrease in a second phase with an apparent rate constant of  $1.3 \times 10^4 \text{ s}^{-1}$ . A final change (not shown) with a rate constant of  $70 \text{ s}^{-1}$  is due to CO recombination and brings the absorbance back to the preflash level. The amplitudes of the phases vary with the initial reduction level of the enzyme, as shown in Table I.

The transient absorbance changes at 605 nm can also be resolved into three phases with rate constants corresponding to those found at 445 nm. The initial part of the kinetic trace is shown in Figure 2, and it corresponds to an increase in absorbance. The rate constant for the first phase is  $1.7 \times 10^5 \text{ s}^{-1}$ , a value somewhat lower than that for the rapid phase observed at 445 nm. Also at 605 nm, the amplitudes of the absorbance changes depend on the initial degree of enzyme reduction (Table I).

A small absorbance change (0.005) is also observed in the fully reduced enzyme at 445 nm, but this has no counterpart at 605 nm. Thus, it probably reflects a structural perturbation

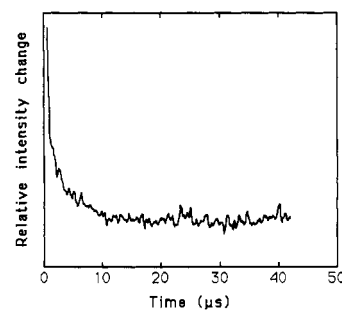


FIGURE 2: Time course of the intensity changes at 605 nm following flash photolysis of mixed-valence carboxycytochrome oxidase ( $5 \mu\text{M}$ ).

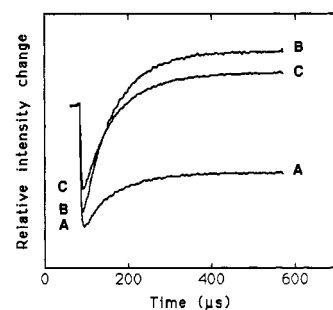


FIGURE 3: Time course of the intensity changes at 830 nm following flash photolysis of carboxycytochrome oxidase ( $30 \mu\text{M}$ ) at different degrees of reduction: (A) 2 electron equiv; (B) 3 electron equiv; (C) 3.5 electron equiv.

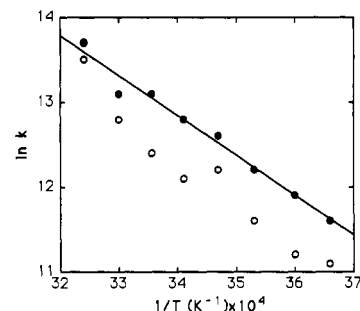


FIGURE 4: Temperature-dependence of the rate constant for the fast phase observed at 445 nm (●) and 605 nm (○). A least-squares fit to the 445-nm data yields the following activation parameters at 298 K:  $\Delta G^\ddagger = 41 \text{ kJ mol}^{-1}$ ;  $\Delta H^\ddagger = 37 \text{ kJ mol}^{-1}$ ; and  $\Delta S^\ddagger = -14 \text{ J K}^{-1} \text{ mol}^{-1}$ .

of cytochrome  $a_3$  on the photodissociation of CO.

The reduction of  $\text{Cu}_A$  was followed at 830 nm, as illustrated in Figure 3. At this wavelength, the initial rapid phase was not observed but only an absorbance decrease with an apparent rate constant of  $1.3 \times 10^4 \text{ s}^{-1}$ , corresponding to the second phase seen at the other wavelengths. The 830-nm changes are appreciable in the mixed-valence enzyme, but the amplitude first increases on further reduction, reaches a maximum at the three-electron-reduction level, then decreases, and disappears in the fully reduced enzyme. The reduction observed at 830 nm is preceded by a lag, which is more pronounced in the mixed-valence enzyme compared to the three-electron-reduced form (Figure 3).

At wavelengths around 600 nm, an absorbance increase with an apparent rate constant of approximately  $400 \text{ s}^{-1}$  was detected (not shown). This can, for example, be seen as a small bump at the beginning of the recombination phase in the trace obtained at 605 nm. The absorbance change at 598 nm is about  $2.5 \times 10^{-3}$  with a  $5 \mu\text{M}$  solution of both the mixed-valence and three-electron-reduced enzyme.

The temperature dependence of the initial rapid phase is shown in Figure 4. The second phase has a very small tem-

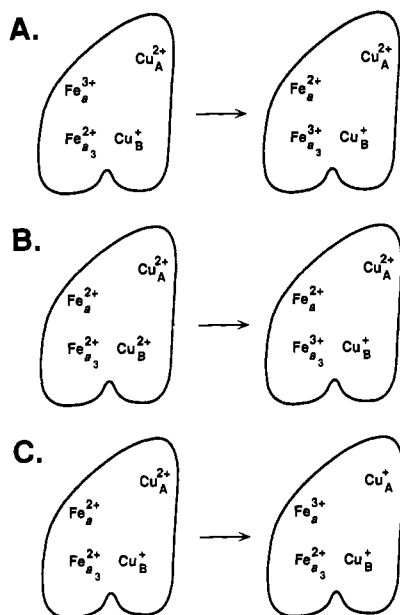


FIGURE 5: Internal electron-transfer reactions in various forms of partially reduced cytochrome oxidase. (A) Main form of mixed-valence oxidase; the same reaction occurs in all forms in which cytochrome  $a_3$  is reduced and cytochrome  $a$  oxidized. (B) Mixed-valence oxidase with  $Cu_B$  oxidized; the same reaction occurs in all forms in which cytochrome  $a_3$  is reduced and  $Cu_B$  oxidized. (C) Three-electron-reduced oxidase; the same reaction occurs in all forms in which cytochrome  $a$  is reduced and  $Cu_A$  oxidized.

perature dependence, but the data are not shown because this phase has been characterized earlier (see Discussion). Within the errors of the measurements, the rapid phase does not vary with pH.

## DISCUSSION

The fast absorbance change (apparent rate constant about  $2 \times 10^5 \text{ s}^{-1}$ ) that we have found at 445 and 605 nm (Figures 1 and 2), but not at 830 nm (Figure 3), with the mixed-valence as well as with the three-electron-reduced enzyme has not been observed earlier. We suggest that it represents ground-state electron transfer between the heme centers of the oxidase. The small amplitudes (Table I) depend on the small difference in reduction potential between these centers. The absorbance change cannot be due to excited-state electron transfer or local heating, because the decay of the vibrational temperature following laser excitation of a heme protein occurs in a few picoseconds (Henry et al., 1986). A structural rearrangement around cytochrome  $a_3$  induced by the photodissociation of CO also appears excluded, since the absorbance change at 605 nm is not seen in the fully reduced enzyme. The small change still observed at 445 nm with the reduced enzyme, on the other hand, probably reflects such a structural perturbation.

Figure 5A gives the reaction that we suggest represents the major part of the fast absorbance change with the mixed-valence enzyme, although it cannot be completely excluded that there is instead electron transfer from  $Cu_B$  to cytochrome  $a$ , followed by very rapid re-reduction of  $Cu_B$  by cytochrome  $a_3$ . It may seem surprising that we observe an absorbance decrease at 445 nm, corresponding to heme oxidation, since it is often stated [see, for example, Brunori et al. (1988)] that cytochrome  $a$  and cytochrome  $a_3$  contribute equally to the reduced - oxidized difference spectra, so that on electron transfer between the cytochromes the net absorbance change would be zero. This is not quite true, however, because the difference extinction coefficient has been estimated to be  $112 \text{ mM}^{-1} \text{ cm}^{-1}$  for cytochrome  $a_3$  and  $57 \text{ mM}^{-1} \text{ cm}^{-1}$  for cytochrome  $a$

Table II: Extent of Reaction<sup>a</sup> following Flash Photolysis of Carboxycytochrome Oxidase

enzyme form	reaction phase	reaction		
		$a_3 \rightarrow a$	$a_3 \rightarrow Cu_B$	$a \rightarrow Cu_A$
mixed valence	1st	0.32	0.1	
	2nd	0.04	0.05	0.1
3-e <sup>-</sup> -reduced	1st	0.22	0.03	
	2nd	0.09	<0.01	0.31

<sup>a</sup> Expressed in micromolar; the total oxidase concentration was normalized to  $5 \mu\text{M}$ .

(Vanneste, 1966; Blair et al., 1982). Thus, on electron transfer from reduced cytochrome  $a_3$  to oxidized cytochrome  $a$  (Figure 5A), one would expect a change in extinction coefficient of  $-55 \text{ mM}^{-1} \text{ cm}^{-1}$ .

The ratio at the two wavelengths for the reaction in Figure 5A should, with the extinction coefficients just given, be 3.5, but we find a ratio of 7 (Table I). There are at least two possible explanations to this apparent discrepancy. One would be extinction interactions between the hemes (Malmström, 1973), making the extinction coefficients used invalid for the particular enzyme states involved here. Even if extinction interactions have been detected (Blair et al., 1982), these are quite small (<10%), making this explanation less plausible.

Another possible explanation is that the mixed-valence oxidase contains a small population of molecules having  $Cu_B$  oxidized and the low-potential centers partially reduced. Flash photolysis would then induce the reaction in Figure 5B in parallel with the reaction in Figure 5A. The sign and magnitude of the absorbance changes in Table I can be fully accounted for, if these parallel reactions occurred (with  $5 \mu\text{M}$  enzyme) to the extent listed in Table II. The fact that there are two parallel reactions could also explain why the rate constants estimated from the traces at 445 and 605 nm differ slightly (Figure 4).

It may seem unlikely that an appreciable fraction of  $Cu_B$  is oxidized in the presence of CO, which raises the reduction potential of the bimetallic site. Our data show, however, that electron redistributions between the high- and low-potential sites are faster than the binding of CO. Thus, some  $Cu_B$  may become oxidized before CO binds to reduced cytochrome  $a_3$ . If electron transfer to  $Cu_B$  always has to go via cytochrome  $a_3$ , it becomes blocked on binding of CO, and  $Cu_B$  remains partially oxidized.

Witt and Chan (1987) have shown that it is possible to prepare a form of the oxidase in which cytochrome  $a_3$  is reduced, with CO bound to it, whereas  $Cu_B$  is fully oxidized. This would be in agreement with our suggestion that  $Cu_B$  may be partially oxidized in the presence of reduced cytochrome  $a_3$ . Unfortunately, it is not feasible to support this hypothesis further with EPR spectra, since it is impossible to detect a  $Cu_B$  signal of a few percent in the presence of close to 100%  $Cu_A$ .

The amplitude of the reaction in the fast phase is decreased in the three-electron-reduced enzyme (Table I). This is expected, since cytochrome  $a$  is reduced in about half of the enzyme population on the time scale of the cytochrome  $a_3$ -cytochrome  $a$  relaxation, in view of the cytochrome  $a$ - $Cu_A$  equilibrium being comparatively slow (see below). Again, it is possible to rationalize the absorbance changes in terms of the reactions in Figure 5A,B with the extents of reaction listed in Table II.

The apparent rate constant determined experimentally for the rapid phase is a function of the forward and reverse rate constants for the reactions in Figure 5A,B. The sum of the rate constants for these two reactions must be very similar, since one rapid phase only is resolved. The reaction in Figure

5A has an equilibrium constant which is far in the direction of reduced cytochrome  $a_3$  and oxidized cytochrome  $a$ . Thus, the observed rate constant should be very close to the true rate constant for the electron transfer from cytochrome  $a$  to cytochrome  $a_3$ . This also justifies the estimation of activation parameters for this reaction from the temperature dependence of the apparent rate constant for the rapid phase (Figure 4).

The second reaction phase, with an apparent rate constant of  $1.3 \times 10^4 \text{ s}^{-1}$ , is seen with both the mixed-valence and the three-electron-reduced enzyme at the three wavelengths used. The fact that the absorbance at 830 nm decreases shows that this phase involves  $\text{Cu}_A$  reduction, and we suggest that it represents the reaction in Figure 5C. This shift in electron distribution is caused by changes in reduction potentials on dissociation of CO (Blair et al., 1986b). The absorbance changes observed (Table I) can be explained, if the reaction in Figure 5C occurred to the extent listed in Table II. As observed (Figure 3, Table I), this reaction is expected to be maximal with the three-electron-reduced enzyme, because here species with cytochrome  $a$  and  $\text{Cu}_A$  partially reduced dominate.

Our second reaction phase is probably identical with reactions observed earlier with the mixed-valence (Boelens et al., 1982; Brzezinski & Malmström, 1987) and with the three-electron-reduced enzyme (Morgan et al., 1989). This agrees with the assignment of Morgan et al. (1989), who were, however, concerned about the fact that more  $\text{Cu}_A$  was reduced than cytochrome  $a$  oxidized. This gets its explanation by our finding that the shift is coupled to the further electron redistribution between cytochrome  $a$  and cytochrome  $a_3$  (Figure 5A). The groups working with the mixed-valence enzyme suggested that cytochrome  $a_3$  rather than cytochrome  $a$  is the direct donor of electrons to  $\text{Cu}_A$ . Our finding of an initial, rapid electron transfer from cytochrome  $a_3$  to cytochrome  $a$  in both enzyme forms makes it instead likely that the same reaction (Figure 5C) is involved. This agrees with the lag observed at 830 nm, since this is most pronounced in the mixed-valence enzyme. The shifts observed (Table II) are also those expected from the established reduction potential interactions between the redox sites (Blair et al., 1986b). Such interactions explain why there is a further shift of electrons from cytochrome  $a_3$  to  $\text{Cu}_B$ , when the redox equilibrium between cytochrome  $a$  and  $\text{Cu}_A$  is established in the second reaction phase. The slow phase ( $400 \text{ s}^{-1}$ ), observed around 600 nm by Brzezinski and Malmström (1987), and also here (see Results), should then represent a structural change rather than electron transfer.

Our finding that the equilibrium between cytochrome  $a$  and  $\text{Cu}_A$  is slower than that between cytochrome  $a$  and the bimetallic site suggests that the normal electron-transfer sequence is  $c \rightarrow \text{Cu}_A \rightarrow a \rightarrow (a_3, \text{Cu}_B)$ . This agrees with some recent work of Hill (1991).

Holm et al. (1987) have constructed a structural model for subunit I of cytochrome oxidase in which cytochromes  $a$  and  $a_3$  are coordinated to the same transmembrane helices [see also Saraste (1990)]. Objections to this model have been raised (Malmström, 1989) on the basis that it would predict a rapid electron transfer between the two cytochromes, whereas it was believed that only  $\text{Cu}_A$  can donate electrons rapidly to the bimetallic site (Brzezinski & Malmström, 1987). Our finding that there is, however, a rapid redox equilibrium between cytochrome  $a$  and the bimetallic site makes the model of Holm et al. (1987) more attractive.

Since all three reactions in Figure 5 are relatively fast, both reduced primary electron acceptors will rapidly transfer electrons to the bimetallic site. The driving force for electron

transfer in the absence of dioxygen is rather modest (Wikström, 1988), which suggests that the free energy of activation ( $41 \text{ kJ mol}^{-1}$ ) is mainly determined by the reorganization energy (Marcus & Sutin, 1985). This probably stems from structural changes in the bimetallic site associated with the electron transfer. Structural changes are also implicated by the negative entropy of activation. The second phase, on the other hand, has a very small reorganization energy [see Brzezinski and Malmström (1987)].

Wikström (1989) has shown that it is only the two-electron transfers from the low-potential sites to the bimetallic site with oxygen intermediates bound which pump protons. Thus, the reactions described here are not directly involved in the proton pump, in agreement with the lack of any appreciable pH dependence of the rates. Rapid electron transfers from  $\text{Cu}_A$  (Oliveberg et al., 1989) and cytochrome  $a$  (Han et al., 1990) have, however, also been observed in the reaction of the reduced enzyme with oxygen. In view of the requirement for electron gating (Blair et al., 1986a), this suggests that in these studies the enzyme has been in the electron-output state. It is then possible that our slowest reaction phase, which we suggested represents a structural change rather than electron transfer, reflects the output-input transition.

#### ACKNOWLEDGMENTS

We thank Dr. Örjan Hansson for his participation in the design of the laser system, in particular, the near-infrared detection device. Mr. Rudolf Jansson constructed a large part of the experimental equipment. Mr. Torbjörn Pascher provided valuable assistance in preparing the figures. Helpful discussions with Dr. Thomas Nilsson and Professor Tore Vänngård are gratefully acknowledged.

#### REFERENCES

- Blair, D. F., Bocian, D. F., Babcock, G. T., & Chan, S. I. (1982) *Biochemistry* 21, 6928–6935.
- Blair, D. F., Gelles, J., & Chan, S. I. (1986a) *Biophys. J.* 50, 713–733.
- Blair, D. F., Ellis, W. R., Jr., Wang, H., Gray, H. B., & Chan, S. I. (1986b) *J. Biol. Chem.* 261, 11524–11537.
- Boelens, R., Wever, R., & Van Gelder, B. F. (1982) *Biochim. Biophys. Acta* 682, 264–272.
- Brautigan, D. L., Ferguson-Miller, S., & Margoliash, E. (1978) *Methods Enzymol.* 53, 128–164.
- Brunori, M., Antonini, G., Malatesta, F., Sarti, P., & Wilson, M. T. (1988) *Adv. Inorg. Biochem.* 7, 93–153.
- Brzezinski, P., & Malmström, B. G. (1987) *Biochim. Biophys. Acta* 894, 29–38.
- Han, S., Ching, Y.-C., & Rosseau, D. L. (1990) *Proc. Natl. Acad. Sci. U.S.A.* 87, 8408–8412.
- Henry, E. R., Eaton, W. A., & Hochstrasser, R. M. (1986) *Proc. Natl. Acad. Sci. U.S.A.* 83, 8982–8986.
- Hill, B. C. (1991) *J. Biol. Chem.* 266, 2219–2226.
- Holm, L., Saraste, M., & Wikström, M. (1987) *EMBO J.* 6, 2819–2823.
- Kobayashi, K., Une, H., & Hayashi, K. (1989) *J. Biol. Chem.* 264, 7976–7980.
- Malmström, B. G. (1973) *Q. Rev. Biophys.* 6, 389–431.
- Malmström, B. G. (1989) *FEBS Lett.* 250, 9–21.
- Malmström, B. G. (1990) *Chem. Rev.* 90, 1247–1260.
- Marcus, R. A., & Sutin, N. (1985) *Biochim. Biophys. Acta* 811, 265–322.
- Morgan, J. E., Li, P. M., Jang, D.-J., El-Sayed, M. A., & Chan, S. I. (1989) *Biochemistry* 28, 6975–6983.
- Oliveberg, M., Brzezinski, P., & Malmström, B. G. (1989) *Biochim. Biophys. Acta* 977, 322–328.

Saraste, M. (1990) *Q. Rev. Biophys.* 23, 331-366.  
 Van Buuren, K. J. H. (1972) Ph.D. Thesis, University of Amsterdam.  
 Vanneste, W. H. (1966) *Biochemistry* 5, 838-848.  
 Wikström, M. (1988) *Chem. Scr.* 28A, 71-74.

Wikström, M. (1989) *Nature* 338, 776-778.  
 Wikström, M., Krab, K., & Saraste, M. (1981) *Cytochrome Oxidase—A Synthesis*, Academic Press, London.  
 Witt, S. N., & Chan, S. I. (1987) *J. Biol. Chem.* 262, 1446-1448.

## Characterization of Covalent Protein Conjugates Using Solid-State $^{13}\text{C}$ NMR Spectroscopy

Joel R. Garbow,\* Hideji Fujiwara, C. Ray Sharp, and Eugene W. Logusch

Monsanto Company, Life Sciences Research Center, St. Louis, Missouri 63198

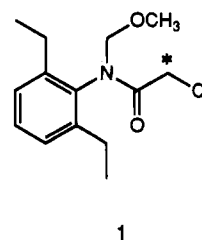
Received January 22, 1991; Revised Manuscript Received April 22, 1991

**ABSTRACT:** Cross-polarization magic-angle spinning (CPMAS)  $^{13}\text{C}$  NMR spectroscopy has been used to characterize covalent conjugates of alachlor, an  $\alpha$ -chloroacetamide hapten, with glutathione (GSH) and bovine serum albumin (BSA). The solid-state NMR method demonstrates definitively the covalent nature of these conjugates and can also be used to characterize the sites of hapten attachment to proteins. Three different sites of alachlor binding are observed in the BSA system. Accurate quantitation of the amount of hapten covalently bound to GSH and BSA is reported. The solid-state  $^{13}\text{C}$  NMR technique can easily be generalized to study other small molecule/protein conjugates and can be used to assist the development and refinement of synthetic methods needed for the successful formation of such protein alkylation products.

Antibody-based immunoassay techniques provide rapid and sensitive methods for the quantitation of small target molecules and are particularly useful as screening methods prior to instrumental analysis of xenobiotic residues in the environment (Wratten & Feng, 1990; Van Emon & Mumma, 1990). In order to elicit antibody production, small molecules must be attached covalently as haptens to carrier proteins. These larger protein conjugates are then used to immunize animals that produce antibodies for immunoassay development. We have been interested for some time in the development of new spectroscopic techniques for the characterization of such small molecule-protein conjugates. We report here on the use of solid-state  $^{13}\text{C}$  NMR spectroscopy as a versatile and effective tool that can be used to characterize hapten-protein conjugates and guide the development of new synthetic approaches for their formation.

Conventional analytical methods such as GC, HPLC, and mass spectrometry are not well suited for characterizing hapten-protein conjugates or for directly detecting covalent bonding between small organic molecules and proteins. While hapten radiolabeling and UV detection have been used to characterize protein alkylation products, no general method short of protein sequencing is available for deriving information about the nature of the attachment (Lundblad & Noyes, 1989). The latter technique is both time consuming and inapplicable to heterogeneous systems such as variably substituted hapten-protein conjugates. Since solid-state  $^{13}\text{C}$  NMR spectroscopy has been used extensively to characterize the structure and dynamics of a variety of synthetic (Fedotov & Schneider, 1989; Komoroski, 1986) and naturally occurring (Garbow & Stark, 1990; Chirlian & Opella, 1990; Garbow et al., 1989; Smith et al., 1989) macromolecular systems, it occurred to us that this technique should be ideally suited to the characterization of hapten-protein conjugates. We con-

sidered that solid-state  $^{13}\text{C}$  NMR, in conjunction with selective hapten  $^{13}\text{C}$  isotope enrichment, could be used for direct observation of nucleophilic protein heteroatom displacement at the  $\alpha$ -position of  $\alpha$ -haloacetyl substrates.



Effective methods for covalently attaching  $\alpha$ -haloacetamides to thiolated protein carriers have recently been developed in our laboratories and were crucial to the elaboration of an immunoassay for the detection of alachlor (1), one of the most widely used of the chloroacetanilide herbicides (Feng et al. 1990a,b). The development of these methods was guided by a powerful new application of solid-state  $^{13}\text{C}$  NMR spectroscopy for the characterization of covalent small molecule-protein conjugates. This NMR technique can provide quantitative measurement of the stoichiometry of hapten-protein conjugation, as well as chemical-shift information useful in identifying the sites of small molecule attachment to proteins. The solid-state  $^{13}\text{C}$  NMR technique thus provides a novel approach for the direct observation and characterization of covalent binding of reactive molecules to proteins and should find wide application for the study of protein modification. In particular, many of the reagents used in protein labeling contain an  $\alpha$ -haloacetyl moiety that reacts with protein nucleophiles via halogen displacement (Lundblad & Noyes, 1989). Furthermore, various strategies for mechanism-based enzyme inactivation ("suicide inhibition") rely on enzyme-catalyzed unmasking of highly reactive  $\alpha$ -haloacetyl al-

\* Author to whom correspondence should be addressed.